

# Kinetic Transformation of Nanofilamentary Au Metal-Metal Composites

K. Wongpreedee\*<sup>1</sup> and A.M. Russell<sup>2</sup>

<sup>1</sup>Division of Materials Science, Department of General Science, Faculty of Science, Srinakharinwirot University, Bangkok, 10110, Thailand.

<sup>2</sup>3109 Gilman Hall, Ames Laboratory, Iowa State University, Ames, IA, 50011, USA.

\* Corresponding author; E-mail: kageeporn@swu.ac.th

## Abstract

**Recovery and recrystallization of Au wire can degrade strength and alter conductivity properties during exposure to elevated temperature. Au Deformation Processed Metal-Metal Composites (Au DMMC's) are being developed for electronic applications requiring high conductivity and high strength. This paper discusses the relationships between microstructure, strength, and resistivity of Au DMMC's. Au DMMC samples were prepared by a powder metallurgy technique and processed into wire down to diameters as low as 120  $\mu\text{m}$ . The extensive deformation reshaped the initially equi-axed powder into filaments that are 30 to 100 nm in diameter and 16 to 180 mm in length, which confers high strength. The high conductivity can be explained by electrons flowing parallel to the filamentary microstructure aligned with the wire axis. Au DMMC's were found to have good thermal stability compared to conventional cold-worked Au interconnection wires. Although these composites will revert to solid solutions if exposed to high temperatures for prolonged times, their relative stability is sufficient to allow them to maintain their two-phase microstructure during the anticipated lifetime temperature profiles of many products.**

## Introduction

High strength and high conductivity are desirable properties for numerous electronic applications. Gold (Au) is frequently used for electronic applications because it possesses high electrical conductivity, excellent ductility, and a contact surface free of oxidation films. During the past two decades, the demand for Au in the electronic industry has increased steadily and currently totals 280 tons per year (1). The largest industrial use of Au in electronics is for interconnection wires. Although other technologies may eventually replace interconnection wires from microprocessor circuits (2, 3), it seems likely that this technology will continue to be widely used for several more years.

The relatively low strength of commercially available Au interconnect wire constrains the minimum wire diameter and pitch that can safely be used in circuit assemblies. Similarly, the limited hardness available in high conductivity Au alloys leads to accelerated wear in electrical switches and connectors. In addition, recovery and recrystallization of Au wire can degrade strength and even conductivity properties during exposure to elevated temperature during wire bonding (up to 250°C for 50 ms) and encapsulation packaging (175°C for 3-6 hours) (4). The present strengthening strategies for Au interconnect wire are limited to cold work processes and additions of various alloying elements at low concentrations (~tens of ppm level). Higher strength and better retention of strength at elevated temperature could be achieved by using higher alloying element concentrations, but higher alloy concentrations raise electrical resistivity to unacceptable levels.

New materials are needed to improve the strength and thermal stability of Au alloy used for interconnection wire and for related applications. Au Deformation Processed Metal Metal Composites (Au DMMC's) are being developed for electronic applications requiring high conductivity and high strength (5, 6). Au-Ag and Au-Pt DMMC's possess an extraordinary combination of properties due to their nanofilamentary microstructure of second phase metals in a Au matrix. Table 1 shows strength and resistivity relations of Au-DMMC's at 550 micron diameter (7). The DMMC microstructure produces a Au-based material of 120 micron diameter with high strength ( $\sigma_{\text{UTS}} = 665 \text{ MPa}$ ) and low electrical resistivity ( $3.07 \mu\Omega\text{-cm}$ ) (8). By comparison, a 20 micron diameter commercial Au interconnect wire, sold by one of the leading suppliers to the semiconductor industry, has 300 MPa tensile strength and  $3.24 \mu\Omega\text{-cm}$  resistivity. These properties suggest that Au DMMC's could be useful materials for interconnect wires, especially in applications such as low-long loop packing (9). It could also solve problems for users of ribbon wires in advanced packages in wireless and optoelectronic applications. However, the

stability of the Au DMMC microstructure must be well characterized to assure reliability for long life-time applications. Concerns arise regarding the effect of heating on the metastable microstructures of Au DMMC's during wire bonding and encapsulation packaging of chips or during the arcing and Ohmic heating that can occur in switch contacts and connectors.

Even though the filaments of Au-Ag and Au-Pt DMMC wire at room temperature show long-term (i.e. years) stability against homogenization by diffusion and against spontaneous morphology changes in the filaments (5), the Au-Ag and Au-Pt equilibrium phase diagrams predict that simple solid solutions are the lowest energy configuration for these materials. In the study reported here, the kinetics of diffusion-driven intermixing of Ag and Pt atoms into the Au matrix in the system of Au-Ag and Au-Pt DMMC's were measured to determine the parameters in the Avrami and Arrhenius equations governing the intermixing (10, 11). Once these values are known, it is possible to predict microstructural transformation rates at the times and temperatures known to exist for various engineering applications. This, in turn, allows prediction of whether these materials can perform satisfactorily in actual engineering service.

## Experimental procedures

### Sample preparation

The samples were prepared by mixing powders to produce Au-14 at%Ag, Au-7 at%Ag, and Au-7 at%Pt powder. These blended powders were formed into green bodies by cold isostatic pressing (CIP). The CIP'ed compacts were sealed for consolidation in annealed Cu cans and then deformed by extruding, swaging, and wire drawing at room temperature. With adjustment for collapse of 30% porosity

in the CIP'ed compacts,  $\eta$  was calculated as  $\eta = 2 \ln(d_o/d_f)$ , where  $d_o$  is the initial wire diameter and  $d_f$  is the final wire diameter. The Au-Pt and Au-Ag rods with Cu sleeves were swaged at room temperature to a deformation true strain of  $\eta = 5.8$ , and the Cu sleeve was then removed by dissolution in  $\text{HNO}_3$  acid. Finally, the sample was drawn to  $\eta = 9.35$  (diameter = 122  $\mu\text{m}$ ). These specimens were stored at room temperature between experimental steps.

The DMMC wires were annealed to study the kinetics of Ag and Pt filamentary dissolution by diffusion into the Au matrix. Isothermal annealing was performed at 290, 300, and 310°C for the Au-14 at%Ag wire; at 287, 300, and 313°C for the Au-7 at%Ag wire; and at 418, 448, and 478°C for the Au-7 at%Pt wire. After each anneal, the degree of transformation from the non-equilibrium to the equilibrium solid solution was determined by electrical resistance measurements performed at room temperature by a standard four-probe potentiometric technique (12, 13).

### Microstructure observation

A JEOL Scanning Electron Microscope (SEM) was used to examine the microstructures of the Au-Ag and Au-Pt DMMC composites. Thermal stability was analyzed to determine the relation between transformation rates and temperature and to observe the evolution of microstructural change accompanying the dissolution reaction.

### Kinetic modeling

In this paper, two basic kinetic equations were used to interpret the measured electrical resistivity changes with the degree of transformation. Firstly, the Johnson-Mehl-Avrami (JMA) equation was assumed to describe the empirical homogeneous solid-state transformation with respect to time and temperature dependence:

**Table 1**

*Comparison of ultimate tensile strength ( $\sigma$ ), resistivity ( $\rho$ ), the ratio ( $\sigma/\rho$ ) for Au-X DMMC's, Au alloys, and pure metallic elements (7)*

Materials	Tensile strength ( $\sigma$ ), MPa	Resistivity ( $\rho$ ), $\mu\Omega\text{-cm}$	Ratio ( $\sigma/\rho$ ), $\text{MPa}/\mu\Omega\text{-cm}$
DMMC:			
Au-7at%Ag	576	2.418	238
Au-14at%Ag	585	2.763	211
Au-7at%Pt	570	2.516	227
Alloys:			
Au-26.2Ag-1.8Ni	345	12.10	29
Au-25Ag-6Pt	415	16.94	24
Au-30Pt	450	22.00	20
Pure Metals:			
Au	234	2.35	100
Ag	345	1.63	212
Cu	290	1.69	171
Pt	234	10.58	22

$$y = 1 - \exp[-(kt)^n] \quad [1]$$

where  $n$  is the power related to the transformation mechanisms, and  $k$  is the transformation rate constant of homogenization at a given annealing temperature. Variable  $y$  is assigned to the physical property kinetic change. The fractions of metastable DMMC's transformed to homogeneous solid solution are defined as:

$$y = \frac{\rho_t - \rho_0}{\rho_{\max} - \rho_0} \quad [2]$$

where  $\rho_0$ ,  $\rho_t$ , and  $\rho_{\max}$  are the resistivity before annealing, after annealing for time  $t$ , and in the homogeneous solid solution condition respectively.

The second equation is determined from the Arrhenius equation to describe the physical interpretation of the diffusion process by using an atomistic model for activation energy. It was assumed that the extent of annealing depends on temperature exponentially as:

$$k = A \exp\left(\frac{-Q}{RT}\right) \quad [3]$$

where  $R$  is the gas constant,  $T$  is absolute temperature,  $A$  is a constant, and  $Q$  is an activation energy. The activation energy,  $Q$ , is the energy required for diffusive motion in these DMMC systems, but the value of  $Q$  is not necessarily the same as the  $Q$  value obtained from single crystal planar diffusion couple experiments, as will be discussed in a later section of this article.

By using two equations, the kinetic parameters reported in the next section can be used to predict the kinetics of the transformation of interest for engineering applications. The results of these computations can then be compared with the behavior of the commercial materials now in use for these applications.

## Results

### Microstructure and physical property relations

The deformation produces second-phase filaments of Ag within a pure Au matrix (see Figs. 1 and 2). The second elements (Ag or Pt) are initially present as roughly equiaxed powder particles  $\sim 5 \mu\text{m}$  in diameter, but the extensive deformation that occurs during wire drawing reshapes them to filaments that are 30 to 100 nm in diameter and 16 to 180  $\mu\text{m}$  in length. The small filament diameter confers high strength on the composite (14, 15).

The high conductivity can be explained by electrons flowing parallel to the filamentary microstructure aligned with the wire axis. In Fig. 3, the resistivity increases with increasing  $\eta$  up to  $\eta=9.3$  for Au-14 at%Ag DMMC, but Au-7 at%Ag and Au-7 at%Pt increase until  $\eta = 8.3$  and then drop

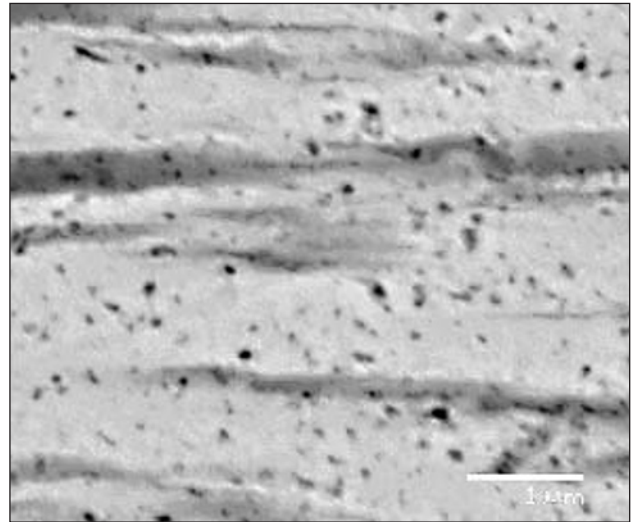


**Figure 1**

Backscattered electron SEM micrograph showing Ag second phase (elongated black phase) starting to form short filaments in the Au matrix for Au-14 at%Ag DMMC at  $\eta = 7.3$ . Energy dispersive spectroscopy (EDS) showed that the small, equiaxed, black regions are SiC abrasive that has become embedded in the sample surface

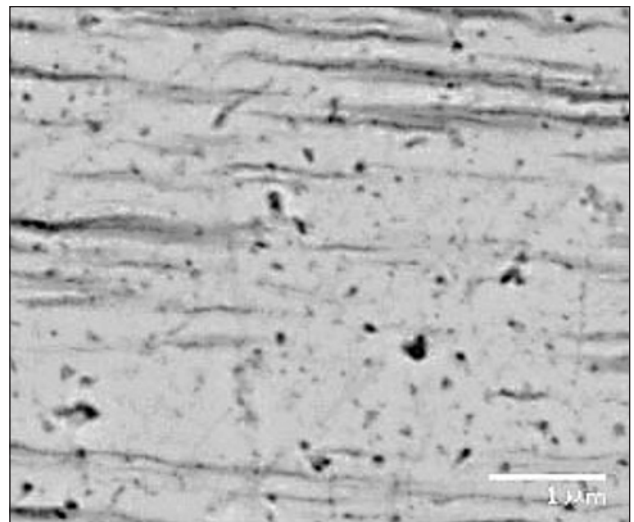


**Figure 2**

Backscattered electron SEM micrograph showing the filamentary microstructure of the Ag second phase (black phase) in the Au matrix for Au-14 at%Ag DMMC. The Ag filaments show longer elongation and smaller diameter at  $\eta = 9.3$ . Note that the filaments microstructure of Au-7 at%Ag and Au-7 at%Pt DMMC are very similar. EDS showed that the small, equiaxed, black regions are SiC abrasive

at the highest deformation level ( $\eta = 9.3$ ). The reason for this behavior at high  $\eta$  is unknown.

### Kinetic transformations

The fractions of the DMMC's transformed from metastable two-phase microstructures to homogeneous solid solutions are depicted by the sigmoidal curves shown in Fig. 4. SEM

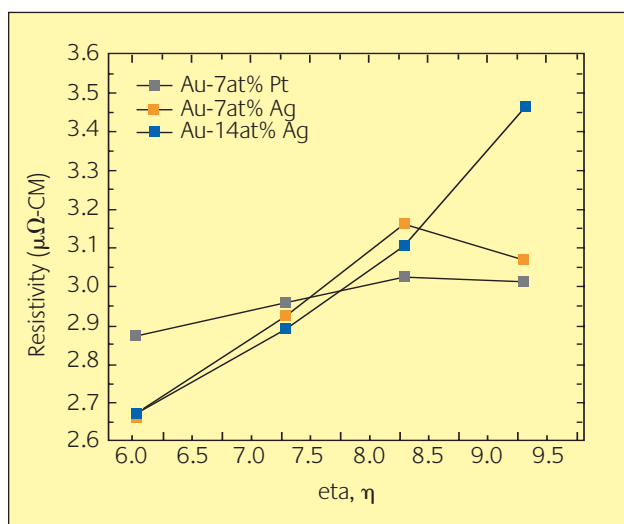


**Figure 3**

The relation between resistivity and deformation true strain. Note that resistivity increases with increasing true strain deformation ( $\eta$ ). Note that the Au-7 at%Ag and Au-7 at%Pt decrease at the highest deformation level, but the Au-14 at%Ag does not

examination shows progressively greater amounts of Ag and Pt dissolution into the Au matrix as annealing time increased (Fig. 5a). For long annealing times at high temperature, Ag filaments become progressively more difficult to discern in SEM micrographs (Fig. 5b) until finally disappearing completely. The data plotted in Fig. 4 were used to

determine the kinetic transformation parameters shown in Table 2. A detailed discussion of the calculation of these parameters is provided elsewhere (10, 11).

The Avrami and Arrhenius equation relationships were used with the values of A and Q determined in this study for Au-Ag and Au-Pt DMMC's to develop the transformation maps in Fig. 6. These plots in time-temperature space predict the extent of high temperature degradation suffered by these materials for various combinations of time and temperature. Fig. 6 shows that Au-7 at%Pt is more resistant to homogenization than the Au-Ag DMMC's, a finding which is consistent with the slower diffusion of Pt in Au *vis-a-vis* Ag in Au.

The area of greatest interest for engineering applications in the maps of Fig. 6 is the region describing the first few percent of transformation. When the DMMC has completed only a few percent of its transformation, it still possesses high strength and high conductivity, but as homogenization proceeds further, the properties degrade sharply, and the material no longer offers advantages over conventional alloys. For this reason, an enlarged view of the early portion of the transformation map is presented in Fig. 7. The map illustrates the temperature and time combinations that cause homogenization ranging from 0 to 3%. As an example, Au-7 at%Pt shows greater thermal stability; calculations predict a 0.1% resistivity increase after 8 days at 175°C or after 17 minutes at 250°C in Fig 6c. Comparing to Au-14 at% in Fig

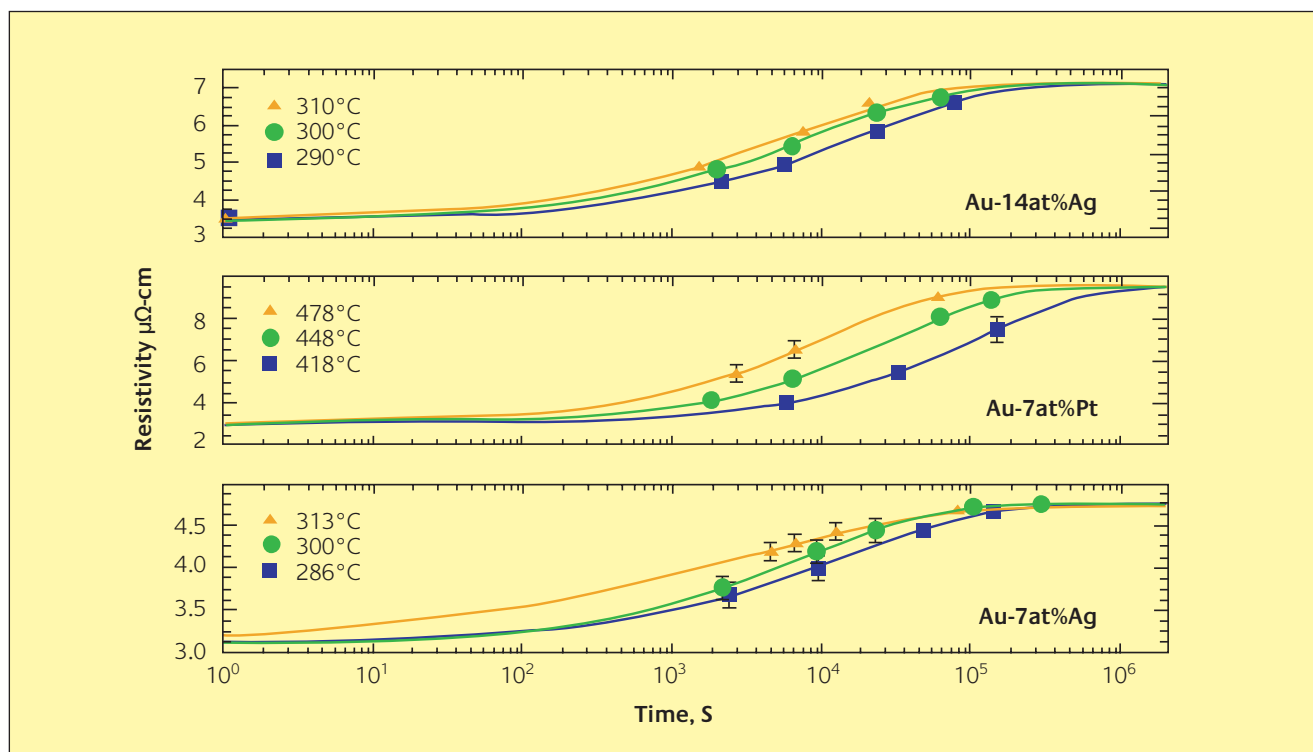


**Figure 4**

Resistivity vs. annealing time plots for Au-14 at%Ag, Au-7at%Ag, and Au-7at%Pt. These sigmoidal curves asymptotically approach the electrical resistivities of the homogeneous solid solutions at the right end of each figure

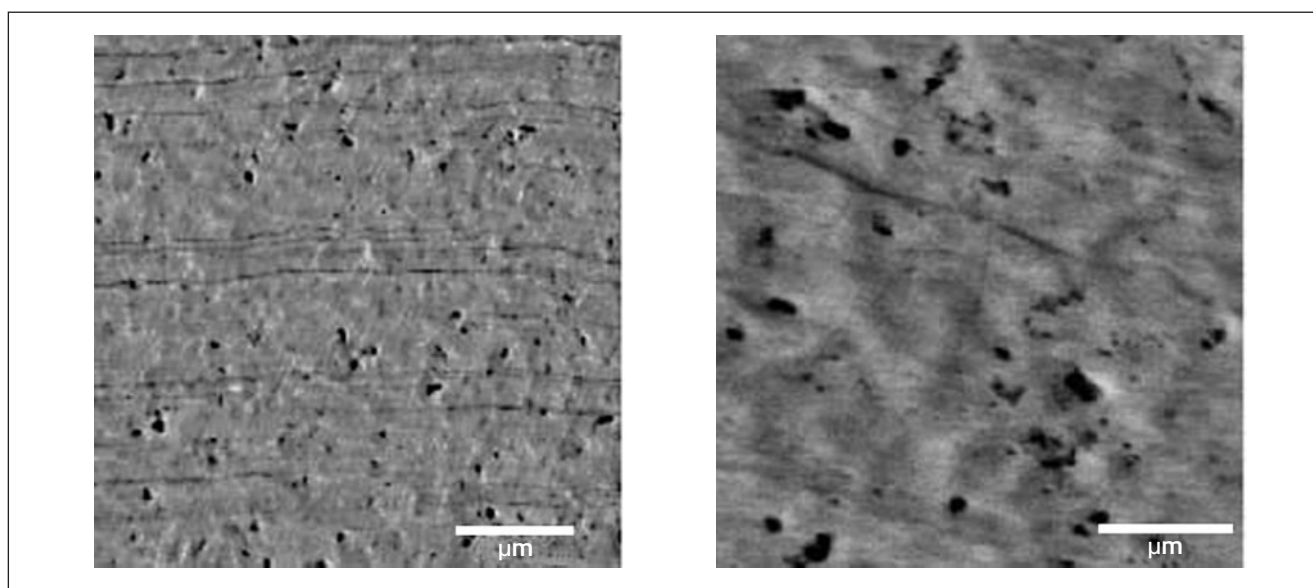


**Figure 5**

SEM backscattered electron images of the microstructure of an Au-14 vol% Ag DMMC. The Ag is visible as dark filaments oriented approximately horizontally in the Au matrix (a) after annealing at 300°C for 1.2 ks. In image (b) an anneal at 300°C for 12.3 ks has partially dissolved the Ag filaments into the Au matrix, and they are more difficult to discern. Note that the magnification for image (b) is higher than for image (a)

**Table 2**

The experimental result of Au-14at%Ag, Au-7at%Ag, and Au-7at%Pt DMMC shows kinetic parameters necessary to calculate the extent of kinetic transformation at various temperatures and times

Sample	Q (kJ/mol)	n	k (s <sup>-1</sup> )	A	Temp(°C)	ref
Au-14 at%Ag	141	0.48	$1.54 \times 10^{-4}$	$7.25 \times 10^8$	290	This study
		0.50	$1.15 \times 10^{-4}$		300	
		0.50	$5.48 \times 10^{-5}$		310	
Au-7 at%Ag	156	0.40	$2.75 \times 10^{-4}$	$2.82 \times 10^9$	287	This study
		0.51	$1.31 \times 10^{-4}$		300	
		0.43	$6.44 \times 10^{-5}$		313	
Au-7 at%Pt	167	0.55	$9.15 \times 10^{-5}$	$4.19 \times 10^7$	418	This study
		0.58	$3.15 \times 10^{-5}$		448	
		0.58	$8.92 \times 10^{-6}$		478	
Au <sup>198</sup> in Ag diffusion couple	202	N/A	N/A	N/A	1073-1205	(16)
Ag <sup>110</sup> in Au diffusion couple	168	N/A	N/A	N/A	800-932	(17)
Au <sup>199</sup> in Pt diffusion couple	252	N/A	N/A	N/A	580-992	(18)
Pt <sup>195</sup> in Au diffusion couple	254	N/A	N/A	N/A	900-1056	(19)

6a, these maps show that a 0.1% resistivity increase (a negligibly small change) is calculated to occur in Au-14 at% Ag after 20 hours at 175°C or after 1.4 s at 250°C. The Au-Ag and Au-Pt DMMC's were found to have better thermal stability than conventional Au interconnection wires. Comparatively, Qi et.al show that cold-worked Au commercial interconnection wire lost strength due to recovery and recrystallization after annealing at 380°C for 1 hour (20).

## Discussion

The shape of the filaments in DMMC's is thought to result from the texture that develops during their deformation processing (21, 22). In DMMC's containing BCC second phase metals, ribbon-shaped filaments form because a <110> fiber texture develops that leaves only two slip directions with non-zero Schmid factors. Once this occurs, the second phase is then restricted in all subsequent deformation to plane strain.



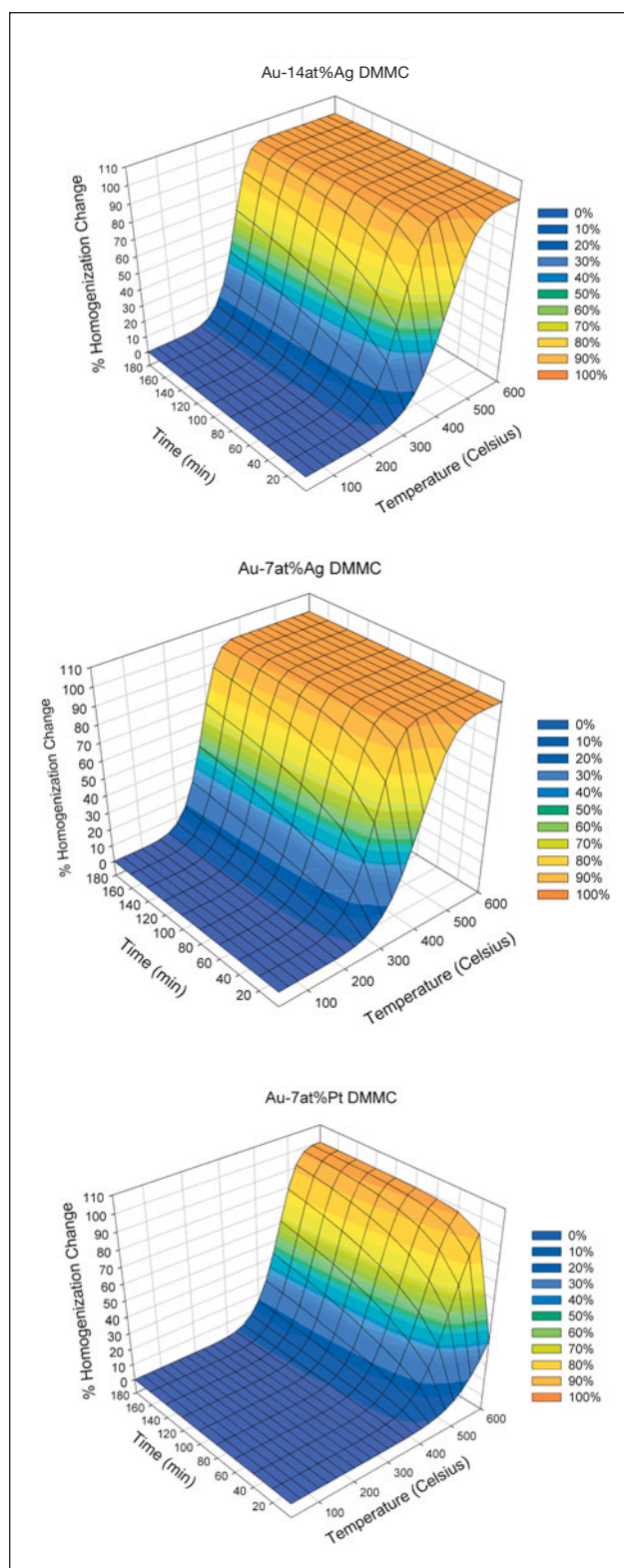


**Figure 6**

Calculated predictions in time-temperature space of the transformation of Au DMMC metastable structures to homogeneous solid solutions. These plots show that Au-7at%Pt is better able to tolerate exposure at high temperature. Au-7at%Pt Au-7at% Ag DMMC is only partially homogenized at combinations of time and temperature which completely homogenize Au-7at%Ag and Au-14at%Ag.

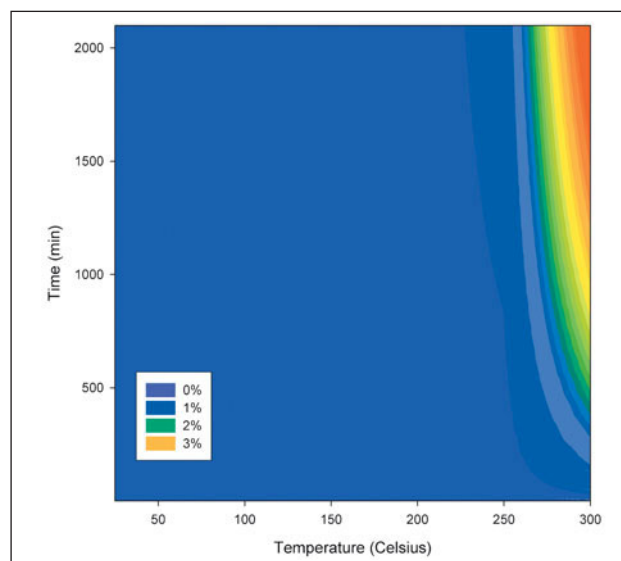


**Figure 7**

Contour map of Au-7at% Pt showing only the most significant time and temperature range for engineering applications such as interconnection wire. Percentages shown in the key are percent change of resistivity

A similar texture effect occurs in DMMC's with HCP second phases. However, in FCC materials such as Ag and Pt, filaments are roughly cylindrical in shape because they have a mixed texture that is partially  $\langle 111 \rangle$  and partially  $\langle 100 \rangle$ . The  $\langle 111 \rangle$  fiber texture leaves three slip directions active, and the  $\langle 100 \rangle$  fiber texture provides four active slip directions during subsequent deformation. Those slip directions are arrayed around the fiber axis, which allows axially symmetric flow resulting in the cylindrical shapes observed in Fig. 1 and 2.

The kinetic transformation involves atomic mobility and thermal activation, which are necessary to overcome the energy barrier to move an atom from one site to another. Table 2 shows that the activation energy measured in this study for the Au DMMC systems is smaller than the activation energy value measured in single crystal, planar diffusion couple Au-Pt and Au-Ag studies (16-19). Diffusional mixing (lower activation energy) occurs more readily in DMMC systems than in single crystal planar interface systems for two reasons: 1) far more defects (dislocations, grain boundaries, vacancies from non-conservative dislocation motion, etc.) are present in the Au-Ag DMMC composite and 2) the small radius of curvature of the Ag and Pt filaments increases the chemical potential for diffusion in the DMMC (10, 11).

## Future work and potential applications

Various experiments would be useful to extend the knowledge base of Au-matrix DMMC's to facilitate their industrial use. These include ball shear tests of DMMC wire

and electromigration for interconnection wire as well as wear resistance of DMMC sheet for switch contacts. When more fully characterized, Au DMMC's may find use in other electronic applications involving elevated temperature service. Many of the demands for strength, wear resistance, reliable connection between component, conductivity, and elevated temperature stability in relays, switch contacts, metal packages, metal-ceramic hybrid packages, and multilayer ceramic interconnects may be met by this new family of Au composites.

## Acknowledgements

The authors are grateful for the financial support provided by Royal Thai Government, Thailand; by Kulicke and Soffa, Inc. of Willow Grove, PA, USA; the International Precious Metals Institute of Pensacola, Florida, USA; and by the Iowa Space Grant Consortium of the US National Aeronautics and Space Administration. This work was performed at Ames Laboratory, operated for the US Department of Energy by Iowa State University under contract no. W-7405-ENG-82. This work has been presented in Gold 2003 conference: New Industrial Applications. The authors also are grateful to Profs. R. Trivedi, L.S. Chumbley, M.J. Kramer, D. Field, and F. Peters for valuable discussions.

## About the Authors

**Dr. Kageeporn** was earned her Ph.D. in Materials Science & Engineering at Iowa State University. Currently, she is a faculty member at Srinakharinwirot University. Her teaching focuses on the metallurgy for jewelry alloys and her research interests involve with structure and mechanical property relation and stability of precious metal and alloys.

**Dr. Russell** is Associate Professor of Materials Science and Engineering at Iowa State University. In addition to his research on deformation processed metal-metal composites, his research interests also include mechanical properties of intermetallic compounds.

## References

- 1 "Gold Survey 2001", Gold Fields Mineral Services ([www.gfms.co.uk](http://www.gfms.co.uk))
- 2 C. Muhlstein, ASTM Standardization News, Nov 1999, 30
- 3 R.R. Tummala, E.J. Rymaszewski, and A.G. Klopfenstein, *Microelectronics Packaging Handbook*, 2nd edition, Chapman & Hall, 1997
- 4 G. G. Harman, *Wire Bonding in Microelectronics; Materials, Process, Reliability, and Yield*, 2nd edition, McGraw-Hill, 1997
- 5 A.M. Russell, K. Xu, L.S. Chumbley, J.J. Parks, and J.L. Harringa, *Gold Bull.*, 1998, **31**(3), 82
- 6 V. Gantovnik, A.M. Russell, L.S. Chumbley, K. Wongpreedee and D. Field, *Gold Bull.*, 2000, **33**(4), 128
- 7 V. Gantovnik, *Micro-Structural Relationships of Heavily Deformed Gold-Silver and Gold-Platinum Composites*, Iowa State University, Ames, IA, M.S. Thesis, 1999
- 8 K. Wongpreedee, IPMI internal report, Ames Laboratory, IA, 2002.
- 9 L. R. Levine, Wire Bonding Optoelectronic packages, *Chip Scale Review*, Nov 2001
- 10 K. Wongpreedee and A.M. Russell, *J. Mat Sci*, to be submitted
- 11 K. Wongpreedee, A.M. Russell, and L.S. Chumbley, *Scripta Mater*, 2003, **49**(5), 399
- 12 S. Hirose, T. Sata, J. Yokata and A. Kamio, *Mater Trans JIM*, 1998, **19**(1), 139
- 13 T. Sato, T. Murakami, Y. Amemiva, H. Hashizume and I. Takahashi, *Acta Metall.*, 1988, **36**(5), 1335
- 14 W.A. Spitzig, A.R. Pelton and F. C. Laabs, *Acta Metall.*, 1987, **35**, 2427
- 15 P.D. Funkenbusch and T.H. Courtney, *Acta metal.*, 1985, **33**(5), 913
- 16 A. Vignes and J.P. Haeussler, *Men. scient. Revue. Metall.*, 1966, **63** (1091), 23
- 17 W.C. Mallard, A.B. Gardner, F. Bass and L.M. Slifkin, *Phys Rev*, 1963, **129**(2), 617
- 18 G. Rein, H. Mehrer, and K. Maier, *Phys. Status Solidii*, 1978, **A45**, 253
- 19 A.J. Mortlock, A.H. Rower, and A.D. Le Claire, *Phil. Mag.*, 1960, **5**, 803
- 20 G. Qi and S. Zhang, *J Mater Process Technol*, 1997, **68**, 288
- 21 A.T. English and G.Y. Chin, *Acta Metall.*, 1965, **13**, 1013
- 22 W.F. Hosford, Jr., *Trans Metall. Soc. AIME*, 1964, **230**, 12